Design for Scientific RENAISSANCE

JASER

Evaluation of "True stress" for Geometrically Nonlinear Plane Stress/Strain Problems

Akasha N. M.[a] And Rahman E. Mohmed[b]
Department of Civil Engineering, Sudan University of Science and Technology, Khartoum, Sudan
[a]nmakasha@yahoo.com, [b]abdulrahman_z@sustech.edu

Article Info

Received: 5th December 2011
Accepted:10th January 2012
Published online: 1st March 2012

ISSN 2231-8844

ABSTRACT

The description of deformation and the measure of strain are essential parts of nonlinear continuum mechanics. In this paper, A new formulation for geometric nonlinear plane stress/strain based on Logarithmic strains (GNLGS) is developed. This is based on the well-known Green's strains and coupled with modifying a formulation based on geometric strains. A geometric nonlinear total lagrangian formulation applied on two-dimensional elasticity using 4-node plane finite elements is used. The formulations are implemented into the finite element program (NUSAP), which is developed for the analysis of plane stress/strain problems subjected to static loading. The solution of nonlinear equations is obtained by the Newton-Raphson method. The program is applied to obtain stresses for the different strain measures. Numerical examples are used to compare the different stresses obtained.

***Key words*: Geometric Nonlinear, stress-strain measures, Logarithmic strain**

1. Introduction

The nonlinearity arises from distinct sources: constitutive nonlinearities and geometric nonlinearities. The former occurs when the stress-strain behavior given by the constitutive relation is nonlinear, where as the latter is important when changes in geometry, whether large or small, have a significant effect on the load deformation behavior. Geometric nonlinearity includes deformation-dependent boundary conditions and loading.

Geometric nonlinearities are introduced by nonlinearities in the kinematics description of the system at hand. The nonlinear strain and stress measures in definition of stress-strain relation are one of the key concepts of several nonlinearities. Strain is known as the change of the shape or geometry produced by applied loads. The loads are defined by the general term stress. To practically assess the stress state on the structure, strain must be measured. There is alternative strain measures used to derive finite element equations, such as Green strain, which is associated with Piola-Kirchoff stress, geometric strain, which is associated with engineering stress, and logarithmic strain, which is associated with true (Cauchy) stress. The Green strain is the most common definition applied to materials used in mechanical and structural engineering problems, which are subjected to small deformations. On the other hand, for some materials, subjected to large deformations, the engineering definition of strain is not applicable (Rees, 2006). Thus, other more complex definitions of strain are required, such as logarithmic strain and Almansi strain.

The geometric (engineering) strain is expressed as the ratio of total deformation to the initial dimension of the material body in which the loads are being applied. Logarithmic strain is the preferred measure of strain used by scientists, who typically refer to it as the "true strain." For large strains, the adopted strain measure is often taken as log-strain, which is of an incremental form. In Lagragian geometric nonlinearity the Cauchy stress (True stress) is associated with logarithmic strains, the Second Piola-Kirchhoff stress is associated with Green's strain, and not to Cauchy stress as was usually assumed (Crisfield, 1997).

In a finite element context, often adopt an updated coordinate system, but maintain the directions of the original rectangular Cartesian system. Thus there will be a need to use a stress measure that relates to this new (or current) system. Even if we adopt a Green's strain/second Piola-Kirchhoff system we may wish to interpret our final stresses in relation to the final geometry because without additional knowledge concerning the deformations, the second Piola–Kirchhoff stresses are difficult to interpret. In very simple terms, the Cauchy stress is (force/final area) rather than (force/original area) and is related to the current configuration, while the second Piola-Kirchhoff stress relates to the original coordinate system configuration.

Ludwik (1909) proposed the Logarithmic strain measure for the one-dimensional extension of a rod with length *l*. It was defined via the integral of *dl/l* to which Ludwik gave the name "effective specific strain." Hencky (1928) extended Ludwik's measure to three-dimensional analysis by defining logarithmic strains for the three principal directions. In their classic treatise in 1960, Truesdell and Toupin (1960) pointed out that all applications of Hencky's logarithmic strain measure had had difficulties because it was complex to evaluate.

Consequently, applications were (up to that point in time) limited primarily to studies wherein the principal axes of strain did not rotate in the body of the structure. With computers now being readily available, this consideration (which was valid in 1960) is no longer a constraint. In their treatise, Truesdell and Toupin (1960) went on to say, "Such simplicity for certain problems, as may result from a particular strain measure, is bought at the cost of complexity for other problems. In a Euclidean space, distances are measured by a quadratic form, and an attempt to elude this fact is unlikely to succeed."

They advocate using the "topological," quadratic strain fields of Almansi (1911) or Green (1841) instead of the "physical," logarithmic strain field of Hencky (1928). A thorough and consistent development of the strain and strain-rate measures affiliated with Hencky was documented (Freed, 1995), and natural measures for strain and strain-rate were expressed in terms of the fundamental body-metric tensors of Lodge. These strain and strain-rate measures, which are mixed tensor fields, were mapped from the body to space in both the Eulerian and Lagrangian configurations and were then transformed from general to Cartesian fields. Then, they were compared with the various strain and strain rate measures found in the literature. A simple Cartesian description for the Hencky strain rate in the Lagrangian state was obtained, but unfortunately, this Cartesian result cannot be integrated (a byproduct of non-unique mappings from general to Cartesian space). Nevertheless, this solution does point the way to obtaining other integrable solutions appropriate for using the Hencky strain to construct constitutive equations.

These investigator (Green, 1841; Almansi, 1911; Hencky, 1928; Truesdell and Toupin, 1960; Freed, 1995) believes that physical, rather than topological, measures of strain, although more complex in evaluation, will ultimately lead to much simpler constitutive equations for describing material behavior, especially under the conditions of large deformations that are often present during material processing.

There are many applications of plane stress/strain in different fields of analysis Pidapati et al. (1989) used large strain 8-node plane stress isoparametric finite element for prediction of rubber fraction. The formulation is based on total Lagrangian description and incremental formulation.

Seki and.Atluri (1994) used 2D plane stress/strain element in application of analysis of strain localization in strain-softening hyper elastic material, using assumed stress hybrid elements.

Fernando (2006) used an assumed strain approach for a linear triangular element based on a total lagrangian formulation and its geometry defined by three nodes with only translational degree of freedom. The strains are computed from the metric tensor, which is interpolated linearly from the values obtained at mid-side points. To deal with plasticity at finite deformation a logarithmic stress-strain pair is used where an additive decomposition of elastic and plastic strains is adopted. A hyper-elastic model for the elastic linear stress-strain relation and isotropic quadratic yield function for plastic part are considered. The element has been implemented into two finite element codes using linear plane stress and nonlinear plane strain problems.

Turner, et al. (1960) reported the finite element procedure to geometrically nonlinear structure. Zienkiwicz (2000) introduced the geometric nonlinear analysis using the total lagragian formulations, with incremental procedure combined with Newton-Raphson (NR) iterative techniques. Mohamed (1983) used both Green strain and geometric strain measures to solve large rotation beam problems. He, also, proposed total lagrangian modified incremental equations for a two- dimensional state of stress based on the geometric strains. This has been adopted as the base for developing the formulation based on the logarithmic strain.

In this paper, geometrically nonlinear formulations based on two-dimensional 4-node plane stress and plane strain isoparametric finite elements are developed. The nonlinear formulations are based on the total Lagrangian formulation and using the Green's strains, Geometric strains and Logarithmic strains. The adopted formulations are implemented into a general-purpose nonlinear finite element program NUSAP and the stresses values obtained from the different strain measures are compared. Numerical examples are used to compare the Piola-kirchoff stresses, the Engineering stresses and the "true" Cauchy stresses.

2. Geometrically Non-linear Finite Element Formulation for Plane Stress/Strain based on Logarithmic Strain

As stated above the geometrically non-linear finite element formulations based on Green's strains and Geometric strains are well established. In this section, the formulation based on Logarithmic strains is out lined.

From the principle of virtual work, the equation can be written in terms of the true Cauchy stresses as:

$$\psi = \int \bar{\boldsymbol{B}}^{\boldsymbol{T}} \sigma d\boldsymbol{v} - \boldsymbol{f} = 0 \tag{1}$$

Where; $\bar{B}^T = B^{*T} S^T = B^T H^T S^T$, $\sigma = D\bar{B}a = DSBa = DSHBa$

In which $\boldsymbol{B}$ is the Green strain matrix, $\boldsymbol{H}$ relates variation in geometric strain to variation in Green's strain and $\boldsymbol{S}$ relates variation in logarithmic strain to variation in Geometric strain, then:

$$\psi = \int_{v} \boldsymbol{B}^{\boldsymbol{T}} \boldsymbol{H}^{\boldsymbol{T}} \boldsymbol{S}^{\boldsymbol{T}} \sigma d\boldsymbol{v} - \boldsymbol{f} = 0 \tag{2}$$

On taking the variation of Eq (2) the results are:

$$\delta\psi = \int_v B^T H^T S^T \delta\sigma dv + \int_v \delta B^T H^T S^T \sigma dv + \int_v B^T \delta H^T S^T \sigma dv + \int_v B^T H^T \delta S^T \sigma dv \tag{3}$$

in which

$$\int_v B^T H^T S^T \delta\sigma dv = \left(\int_v B^T H^T S^T DSHB dv \right) \delta a = \left(K_o + K_L \right) \delta a \tag{4}$$

where

$$K_o = \int_v B_o^T H^T S^T DSHB_o dv \tag{5}$$

$$K_L = \int_v B_o^T H^T S^T DSHB_L dv + \int_v B_L^T H^T S^T DSHB_o dv + \int_v B_L^T H^T S^T DSHB_L dv \tag{6}$$

Since: $B^T = B_o^T + B_L^T$

Then: $\delta B^T = \delta B_L^T = G^T \delta A^T$

Therefore $\int_v \delta B^T H^T S^T \sigma dv = \int_v G^T \delta A^T H^T S^T \sigma dv$ and

$$A^T H^T S^T \sigma' = \begin{bmatrix} \frac{\partial u}{\partial x}\left[\frac{\sigma_x'}{(1+2\varepsilon_x)^{\frac{1}{2}}(1+\varepsilon_x')} - \frac{3\gamma_{xy}\tau_{xy}'}{(1+\varepsilon_x')(1+2\varepsilon_x)^{\frac{3}{2}}(1+2\varepsilon_y)^{\frac{1}{2}}}\right] + \frac{\partial u}{\partial y}\left[\frac{\tau_{xy}'}{(1+\gamma_{xy}')(1+2\varepsilon_x)^{\frac{1}{2}}(1+2\varepsilon_y)^{\frac{1}{2}}}\right] \\ \frac{\partial v}{\partial x}\left[\frac{\sigma_x'}{(1+2\varepsilon_x)^{\frac{1}{2}}(1+\varepsilon_x')} - \frac{3\gamma_{xy}\tau_{xy}'}{(1+\varepsilon_x')(1+2\varepsilon_x)^{\frac{3}{2}}(1+2\varepsilon_y)^{\frac{1}{2}}}\right] + \frac{\partial v}{\partial y}\left[\frac{\tau_{xy}'}{(1+\gamma_{xy}')(1+2\varepsilon_x)^{\frac{1}{2}}(1+2\varepsilon_y)^{\frac{1}{2}}}\right] \\ \frac{\partial u}{\partial y}\left[\frac{\sigma_y'}{(1+2\varepsilon_y)^{\frac{1}{2}}(1+\varepsilon_y')} - \frac{3\gamma_{xy}\tau_{xy}'}{(1+\varepsilon_y')(1+2\varepsilon_x)^{\frac{1}{2}}(1+2\varepsilon_y)^{\frac{3}{2}}}\right] + \frac{\partial u}{\partial x}\left[\frac{\tau_{xy}'}{(1+\gamma_{xy}')(1+2\varepsilon_x)^{\frac{1}{2}}(1+2\varepsilon_y)^{\frac{1}{2}}}\right] \\ \frac{\partial v}{\partial y}\left[\frac{\sigma_y'}{(1+2\varepsilon_y)^{\frac{1}{2}}(1+\varepsilon_y')} - \frac{3\gamma_{xy}\tau_{xy}'}{(1+\varepsilon_y')(1+2\varepsilon_x)^{\frac{1}{2}}(1+2\varepsilon_y)^{\frac{3}{2}}}\right] + \frac{\partial v}{\partial x}\left[\frac{\tau_{xy}'}{(1+\gamma_{xy}')(1+2\varepsilon_x)^{\frac{1}{2}}(1+2\varepsilon_y)^{\frac{1}{2}}}\right] \end{bmatrix}$$

where $\varepsilon_x, \varepsilon_y, \gamma_{xy}$ are Green strains and $\varepsilon_x', \varepsilon_y', \gamma_{xy}'$ are the logarithmic strains.

$$A^T H^T S^T \sigma' = P^* \theta \tag{7}$$

Where, $\theta = \left\{ \frac{\partial u}{\partial x} \frac{\partial v}{\partial x} \frac{\partial u}{\partial y} \frac{\partial v}{\partial y} \right\}^T$, is the vector containing displacement derivatives w.r.t. Cartesian coordinates, and it is related to the nodal displacement by the form: $\theta = Ga$, G is a matrix containing shape function derivatives. Therefore, Eq (7) can written as:

$A^T H^T S^T \sigma = P^* \theta = P^* G a$, where P^* is the initial stress matrix (symmetric matrix), Hence taking variation results in:

$\delta A^T H^T S^T \sigma = P^* G \delta a$, therefore:

$$\int_v \delta B^T H^T S^T \sigma dv = \int_v G^T \delta A^T H^T S^T \sigma dv = \left(\int_v G^T P^* G dv \right) \delta a = K_\sigma \delta a \tag{8}$$

Where; $K_\sigma = \int_v G^T P^* G dv$ is the initial stress stiffness matrix. Also:

$$\delta H^T \sigma' = L \begin{bmatrix} \delta \varepsilon_x \\ \delta \varepsilon_y \\ \delta \gamma_{xy} \end{bmatrix}$$

where

$$\sigma' = S^T \sigma \tag{9}$$

which are the true (Cauchy) stresses. In simple form, Eq (9) can be written as

$$\delta H^T \sigma' = T' \delta \varepsilon = T' B \delta a \tag{10}$$

Where T' is second initial stress matrix.(symmetric matrix)

$$\int_v B^T \delta H^T \sigma' \sigma dv = \left(\int_v B^T T' B dv \right) \delta a = K_\sigma^* \delta a \tag{11}$$

Where $K_\sigma^* = \int_v B^T T' B dv$ is additional initial stress stiffness matrix

Similarly $H^T \delta S \sigma = M^* B \delta a$

where M^* is the a third initial stress matrix and is given in terms of the initial stresses and strains, therefore:

$$\int_v B^T H^T \delta S^T \sigma dv = \left(\int_v B^T M^* B dv \right) \delta a = K_\sigma^{**} \delta a \tag{12}$$

where K_σ^{**} is the second additional initial stress stiffness matrix

From Eqs. (4), (5), (6), (11) and (12) the tangent stiffness matrix due to logarithmic strains can be defined by:

$$\delta \psi = \left(K_o + K_L + K_\sigma + K_\sigma^* + K_\sigma^{**} \right) \delta a = K_{TL}^* \delta a \tag{13}$$

Where $K_{TL}^* = K_o + K_L + K_\sigma + K_\sigma^* + K_\sigma^{**}$ is the tangent stiffness matrix due to logarithmic strains

Using the residuals $\delta \psi$, equation (13) is used to obtain the incremental displacements. These are then used to obtain the incremental strains and strains in each element.

3. Numerical Results and Discussion:

The finite element formulation described in the above section was implemented in the FORTRAN based NUSAP. Two numerical examples of large deformation problems were

examined to demonstrate the degree of accuracy that can be obtained by using the geometrically non-linear formulations based on 4-node isoperimetric plane stress/strain element by using Green's strains, geometric strains and the new formulation, namely logarithmic strains. The results of stresses of the different strain measures are obtained and compared.

3.1 Cantilever under Pure Bending at Free End:

A cantilever subjected to pure moment is considered. The cantilever is of dimensions L =3000mm, D =300mm and thickness t =60mm as shown in Fig.1.

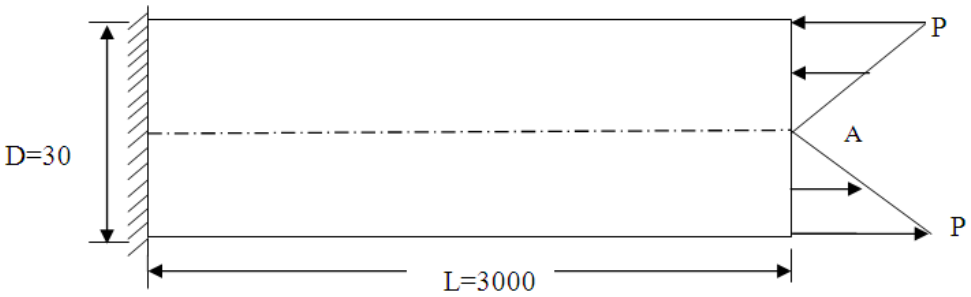

Fig.1. Cantilever under pure bending

The numerical values of material property parameters are Young's modulus, E =210 GPa, and Poisson's ratio, υ =0.3. The structure is modeled with a mesh of 40-isoparametric elements, and the integration order is 2×2. The mesh is of equal size elements of 150×150mm. Results are presented in Figs. (2-5) and tables (1) and (2).

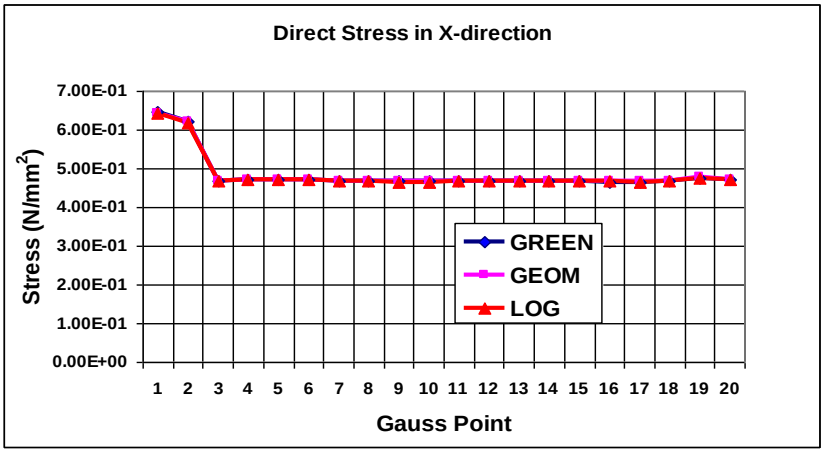

Fig.2. Direct Stress in X-direction, at minimum load=3000N

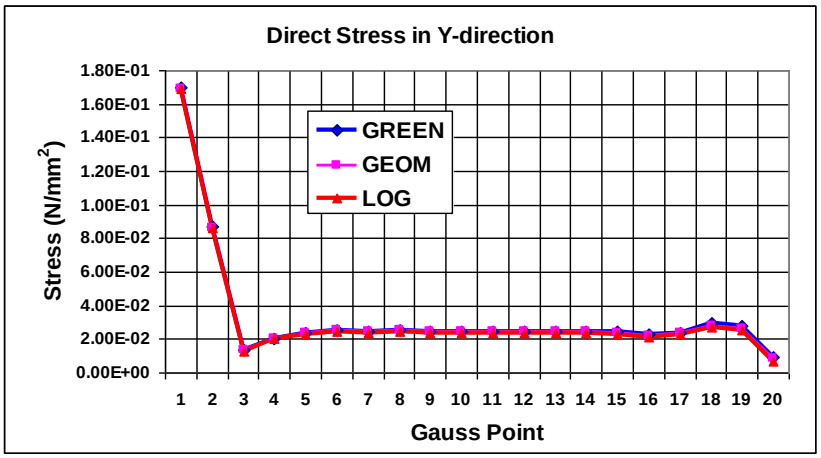

Fig.3. Direct Stress in Y-direction, at minimum load=3000N

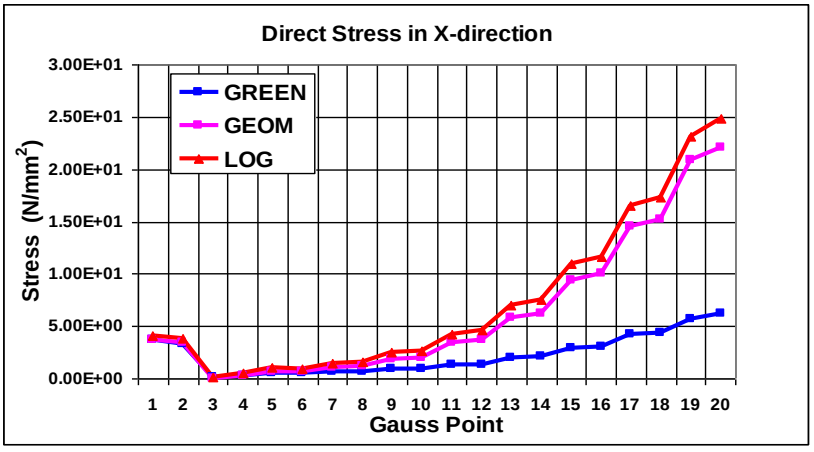

Fig.4. Direct Stress in X-direction, at maximum load=30000N

Table 1: Direct stress in x-direction, at minimum load=3000N

GAUSS POINT	GREEN	GEOM	LOG	GAUSS POINT	GREEN	GEOM	LOG
1	0.648	0.645	0.644	11	0.467	0.468	0.467
2	0.623	0.620	0.620	12	0.467	0.468	0.466
3	0.469	0.470	0.469	13	0.467	0.468	0.467
4	0.472	0.472	0.471	14	0.467	0.468	0.467
5	0.472	0.472	0.471	15	0.466	0.468	0.467
6	0.473	0.473	0.472	16	0.466	0.467	0.466
7	0.468	0.468	0.467	17	0.465	0.467	0.466
8	0.468	0.468	0.467	18	0.467	0.468	0.467
9	0.466	0.467	0.466	19	0.476	0.477	0.475
10	0.466	0.467	0.466	20	0.470	0.472	0.470

Table 2: Direct stress in y-direction, at maximum load=30000N

GAUSS POINT	GREEN	GEOM	LOG	GAUSS POINT	GREEN	GEOM	LOG
1	1.990	1.930	1.910	11	0.554	2.250	2.990
2	1.010	1.010	0.927	12	0.792	3.170	4.040
3	0.045	0.103	0.070	13	1.160	4.490	5.550
4	0.157	0.192	0.007	14	1.510	5.890	7.110
5	0.226	0.224	0.012	15	2.050	7.890	9.310
6	0.156	0.066	0.221	16	2.540	9.850	11.400
7	0.057	0.137	0.487	17	3.180	12.500	14.300
8	0.013	0.435	0.854	18	3.760	15.000	17.300
9	0.162	0.876	1.390	19	5.170	19.700	22.200
10	0.314	1.440	2.050	20	7.240	25.200	27.500

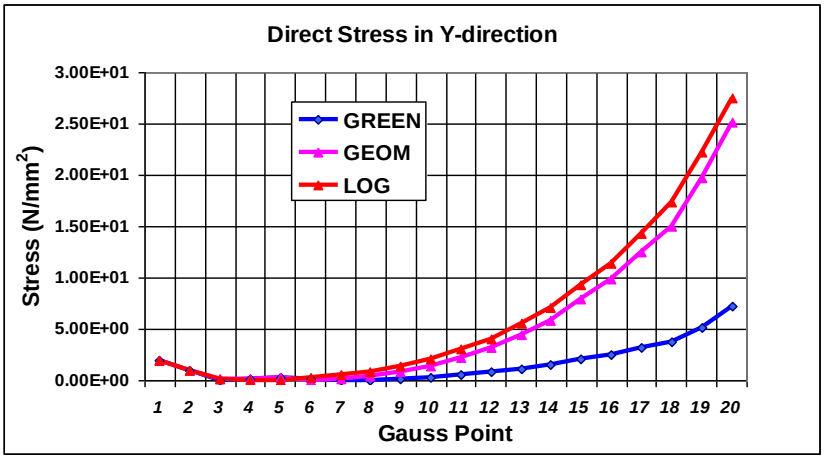

Fig.5. Direct Stress in Y-direction, at maximum load=30000N

Direct stresses obtained in x-and y-directions are shown in Figs. (2).and (3), from which it is observed that the stress distributions resulting from applying the lower load of (3000N) are entirely the same and identical. When the maximum load (30000N) is applied, the results of direct stresses, as depicted in Table (2) show that there is a slight difference in stresses obtained using geometric and logarithmic strain while those obtained from Green's strain give smaller values of stress as shown graphically in Figs.(4) and (5). Also the engineering and true stress values increase continuously with increase in load.

3.2 Clamped beam under point force

A beam with two-fixed ends is considered. The beam is of length L =200mm, height b =10mm and thickness 1mm as shown in Fig. 6. The numerical values for material property parameters are Young's modulus, E =210GPa, Poisson's ratio, υ =0.3. The beam is modeled with mesh of 20-elementes, the integration order used is 2×2.

The computed results of the stresses at the centre point A, and at support (point 1) from the three formulations are obtained and compared.

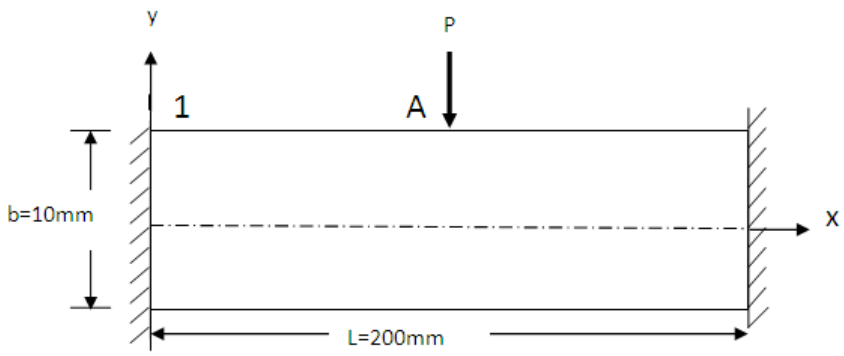

Fig.6. Clamped beam under point force

This example was analyzed by applying 45 load increments. The results obtained show that at the early stages of load, the three formulations curves are coincident then a variation between them is observed, and the log-curve resulted in a tendency to give infinite result for maximum load as expected. Figs (7 to 9) are plotted as a result to show the relation between load increments and average nodal stress at mid span of the beam (point A).

The relation between the average nodal stress in x-direction and load increments is shown in Fig (7). The figure shows that there is a similarity between log and geometric curves, while, a noticeable difference is observed between the Green's and the other two curves. Fig (8), which is the relation between load increments and average nodal stress in y-direction, shows a slight difference between geometric and log strain measures, but the Green's strain measure shows a different trend. This indicates that Engineering stress result in good measure of stress, and resembles closely the true stress.

In case of shear stress in xy-direction it is found that, in the early load increments, the values of shear stress are zero. Then with the increase in load the log and geometric curves give a continuously increasing response, while the Green's curve shows different trend and results in small values of stresses as shown in Fig (9).

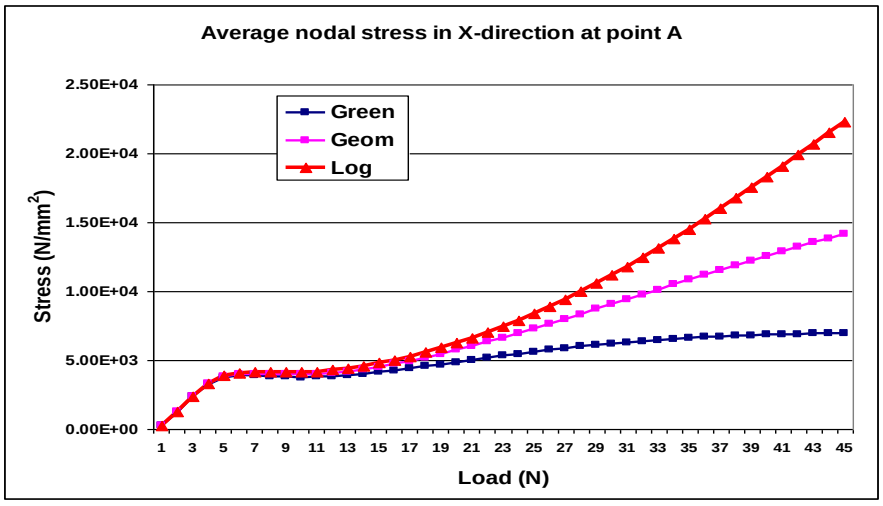

Fig.7. Average nodal stress in x-direction at point A

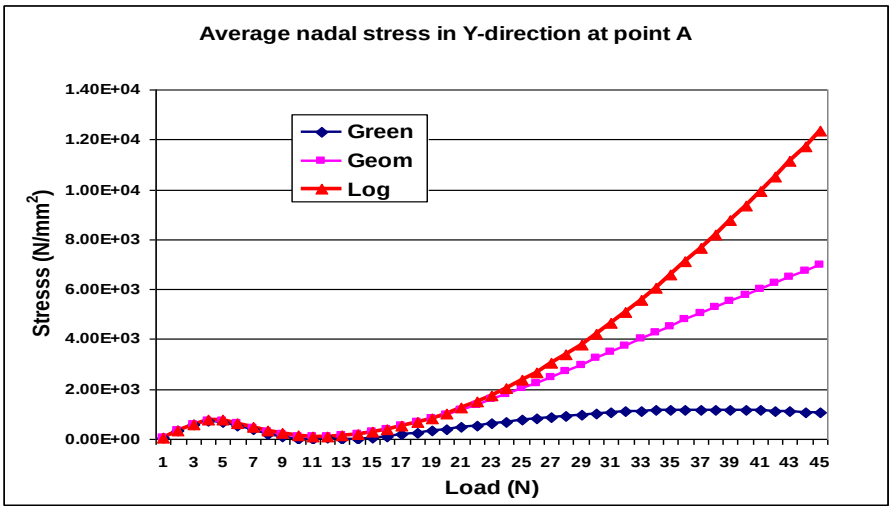

Fig.8. Average nodal stress in y-direction at point A

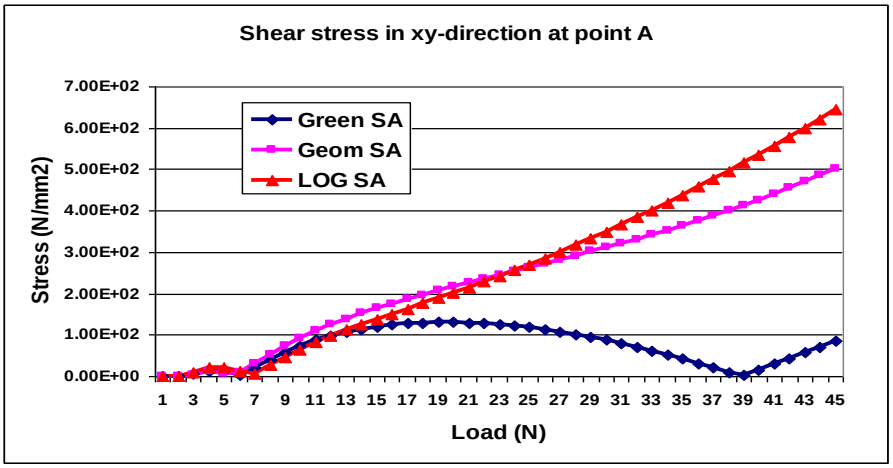

Fig.9. Average nodal stress in xy-direction at point A

For the fixed end of the beam (node1) the results obtained show that there is a difference between log and geometric and the maximum values of stresses are shown by the log curve, and the minimum values of stresses are represented by the Green's curve as shown graphically in Figs (10 and 11).

The shear stress in node 1 is different from that in mid span of beam (node A) as shown in Fig.9, in that the relation of load increments and shear stress values are nonzero in the early stages of load increments as shown in Fig (12). This means that the assumption of zero shear stress at the fixed end of beam is not valid in this case. Then for the next stages of the load there is continuous increase and the maximum values of shear stress are given by the logarithmic formulation.

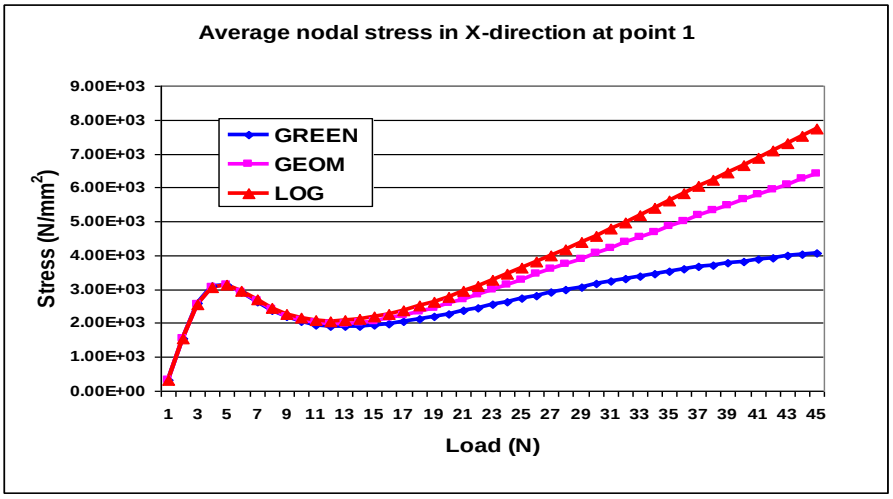

Fig.10. Average nodal stress in x-direction at point1

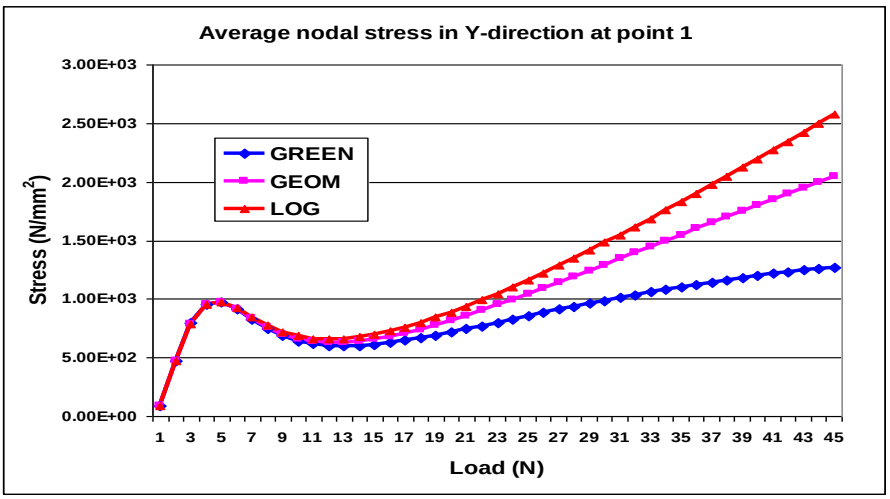

Fig.11. Average nodal stress in y-direction at point1

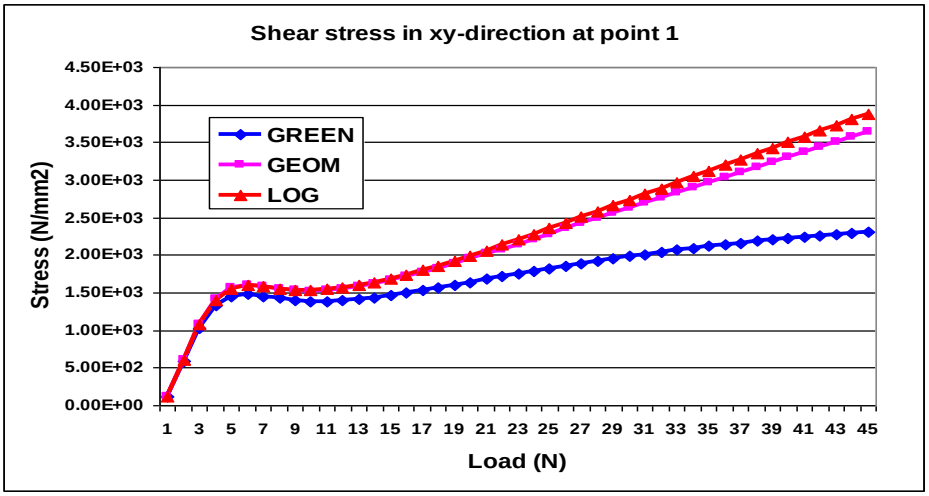

Fig.12. Average nodal stress in xy-direction at point1

4. Conclusions

a. It is found that, for a clamped beam subjected to central load increments the resulting stresses are identical in the early stages of load for the three formulations. Variations occur as load increases and the GNLGS tends to give infinite values of stress for maximum load as expected.
b. It is also found that the assumption of the zero shear stress at fixed end of beam, in the early stages of load, is not valid, whereas in the mid span of the beam it is valid.
c. From all examples carried out in this paper, it is observed that the GNLGS results in high values of stress. This observation is mainly due to the fact that the Cauchy stress is (load/final area) rather than (load/original area) and is related to the current configuration while the Engineering and Piola-Kirchhoff stresses are related to the original configuration.
d. The logarithmic strain formulation can be used when the true stresses are required.

References

Almansi, E. (1911), Sulle deformazioni finite dei solidi elastici isotropi", I. Rendiconti della Reale Accademia dei Lincei, Classe di scienze fisiche, matematiche e naturali, Vol. 20, p. 705-714.

Crisfield, M.A. (1997), Non-linear Finite Element Analysis of solids and structures", Volume2: Advanced Topics, John Wiley & Sons, 1997.

Fernando, F. G.,(2006), A two-Dimensional Linear Assumed Strain Triangular Element for Finite Deformation analysis", American Society of Mechanical Engineers, Vol. 73, 6-970.

Freed, A.D. (1995), Natural Strain. J. Eng. Mater. Technol., Vol. 11 Oct.1995, pp.379385.

Green, G. (1814), On the Propagation of Light in Crystallized Media". Trans. Cambridge Phil. Society, vol. 7, pp. 121-140.

Hencky, H., (1928), Uber die Form des Elastizitatsgesetzes bei ideal elastischen Stoffen.Zeit. Tech. Phys., vol. 9, 1928, pp. 215-220, 457.

Ludwik, P. (1909), Elemente der Technologischen Mechanik". Applied Mechanics, Verlagvon J. Springer, Berlin.

Mohamed, A. E. (1983), A small Strain Large Rotation Theory and Finite Element Formulation of Thin Curved Beam, Ph.D. Thesis, The City University, London, 1983.

Pidapati, R. M. V. Yang T. Y. and Werner Soedel, (1989), A plane Stress Finite Element Method for Prediction of Rubber Fracture", Int. J. of fracture, vol. 39, No 4,pp. 255-268.

Rees, David W.A.,(2006), Basic Engineering Plasticity- An Introduction with Engineering and Manufacturing Application", Butterworth-Heinemann..

Seki, W., and Atluri S. N., (1994), Analysis of Strain Localization in Strain-Softening Hyperelastic Materials, using Assumed Stress Hybrid Element",Computational Mechanics Centre, Atlanta, Georgia, No.14,pp. 549-585.

Truesdell, C., and Toupin, R. (1960), The Classical Field Theories. Encyclopedia of Physics", Vol. III/1, S. Flugge (ed), Springer-Verlag, Berlin, 1960, pp. 226-793.

Turner, M. J., Dill E. H., Martin H. C. and Melosh R, J, (1960),Large deflection of structures subject to heating and external load", J. Aero. Sci., 27, 97-106.

Zienkiewicz, O. C. and Taylor R. L. (2000), The Finite Element Method, Vol.2, fifth edition, Butterworth-Heinemann